BIOELECTRICITY
Volume 3, Number 1, 2021

DOI: 10.1089/bioe.2020.0048

Directional Migration of Breast Cancer Cells Hindered by Induced Electric Fields May Be Due to Accompanying Alteration of Metabolic Activity

Travis H. Jones, PhD,[1,3,*] Kirti Kaul, PhD,[2,3,*] Ayush A. Garg, PhD,[1,*] Jonathan W. Song, PhD,[1,3] Ramesh K. Ganju, PhD,[2,3] and Vish V. Subramaniam, PhD[1,3]

Abstract

Background: Induced electric fields (iEFs) control directional breast cancer cell migration. While the connection between migration and metabolism is appreciated in the context of cancer and metastasis, effects of iEFs on metabolic pathways especially as they relate to migration, remain unexplored.
Materials and Methods: Quantitative cell migration data in the presence and absence of an epidermal growth factor (EGF) gradient in the microfluidic bidirectional microtrack assay was retrospectively analyzed for additional effects of iEFs on cell motility and directionality. Surrogate markers of oxidative phosphorylation (succinate dehydrogenase [SDH] activity) and glycolysis (lactate dehydrogenase activity) were assessed in MDA-MB-231 breast cancer cells and normal MCF10A mammary epithelial cells exposed to iEFs and EGF.
Results: Retrospective analysis of migration results suggests that iEFs increase forward cell migration speeds while extending the time cells spend migrating slowly in the reverse direction or remaining stationary. Furthermore, in the presence of EGF, iEFs differentially altered flux through oxidative phosphorylation in MDA-MB-231 cells and glycolysis in MCF10A cells.
Conclusions: iEFs interfere with MDA-MB-231 cell migration, potentially, by altering mitochondrial metabolism, observed as an inhibition of SDH activity in the presence of EGF. The energy intensive process of migration in these highly metastatic breast cancer cells may be hindered by iEFs, thus, through hampering of oxidative phosphorylation.

Keywords: induced electric field, electrotransductive migration, MDA-MB-231, MCF10A, metabolic activity

Introduction

Cell migration plays a critical role in the physiology of embryonic development and wound healing and also contributes to the pathology of cancer through metastasis.[1,2] Bioelectric effects greatly impact cell migration,[1,3,4] although the distinct effects of electric fields (EF) alone versus EF in the presence of electrical current flow remain to be better understood.[5–7] The recent use of time-varying magnetic fields to induce asymmetric noncontact EFs via Faraday's law has revealed previously unexplored phenomena termed electrotransductive migration.[8,9] These induced electric fields (iEFs) affect spontaneous migration (i.e., in the absence of a chemoattractant) as well as migration stimulated by a biomolecular gradient of epidermal growth factor (EGF) and CXCL12 (or SDF-1α).[8,9] Asymmetric iEFs alter average migration speeds (averaged over 12 h) of both MDA-MB-231 breast cancer cells and nontransformed, normal MCF10A breast epithelial cells in a direction-dependent manner as well as reduce the number of migrating cells in the presence of EGF gradients.[8,9] Importantly, in the absence of EGF, MCF10A cells do not migrate with and without iEFs. Specific to MDA-MB-231 cells, iEFs inhibited epidermal growth factor receptor (EGFR) phosphorylation and altered the remodeling of the actin cytoskeleton in the presence of EGF.[9] In contrast, no changes in EGFR phosphorylation or actin cytoskeleton were observed for MCF10A cells in the presence of EGF. Finally, the Akt pathway was shown to play a vital role as inhibition of Akt nullified the directional effects of iEF.

[1]Department of Mechanical and Aerospace Engineering, The Ohio State University, Columbus, Ohio, USA.
[2]Department of Pathology, College of Medicine, The Ohio State University, Columbus, Ohio, USA.
[3]Comprehensive Cancer Center, The Ohio State University, Columbus, Ohio, USA.
*All three authors contributed equally to this work.

Numerous processes involved in cell migration, including actomyosin contraction, focal adhesion point breaks, and actin polymerization, are known to be energy intensive processes that rely primarily on mitochondrial respiration.[10] Migration characteristics such as cell speed and net displacement have been shown to be dependent on ATP:ADP ratio in a cell.[10,11] While other energetic pathways such as glycolysis and pentose phosphate shunt also contribute to supplying the cell with energy, mitochondrial oxidative phosphorylation is the major contributor.[10] Moreover, mitochondrial function also controls Ca^{2+} channels[12,13] and reactive oxygen species generation, both of which act as secondary messengers in the pathways involved in cell migration, both in physiologically normal and cancer cells.[14,15] Although conventionally considered glycolytic, most cancer cells meet their energy needs through mitochondrial function.[8] Furthermore, the significance of the mitochondrial respiratory enzyme succinate dehydrogenase (SDH) (Complex II of the electron transport chain) is best appreciated when considering tumors bearing mutations in SDH.[16,17] Several studies on MDA-MB-231 cells targeting mitochondrial fusion or fission have found a significant reduction in cell migration, invasion, and proliferation.[18]

A retrospective analysis was conducted on recently reported average speed data during migration for these two cell lines (MDA-MB-231 metastatic breast cancer cells and nontransformed, ''normal'' breast epithelial cells) in the presence/absence of noncontact iEFs and EGF.[9] Detailed examination of momentary migration (over 30 min intervals) rather than average migration over the 12 h duration of the experiments reveals that iEFs increase forward migration speeds while also increasing instances of slow migration or stagnation. These occasions of slow migration or stagnation primarily occur when cells attempt movement in the reverse direction (Fig. 1). The different migratory behaviors exhibited by metastatic versus normal cells in response to iEFs as well as the importance of Akt signaling, point to the possible role of underlying energetics as dictated by metabolic processes.[9] The role of EFs in modulating the metabolic activities of migrating cells, however, has not been fully explored.

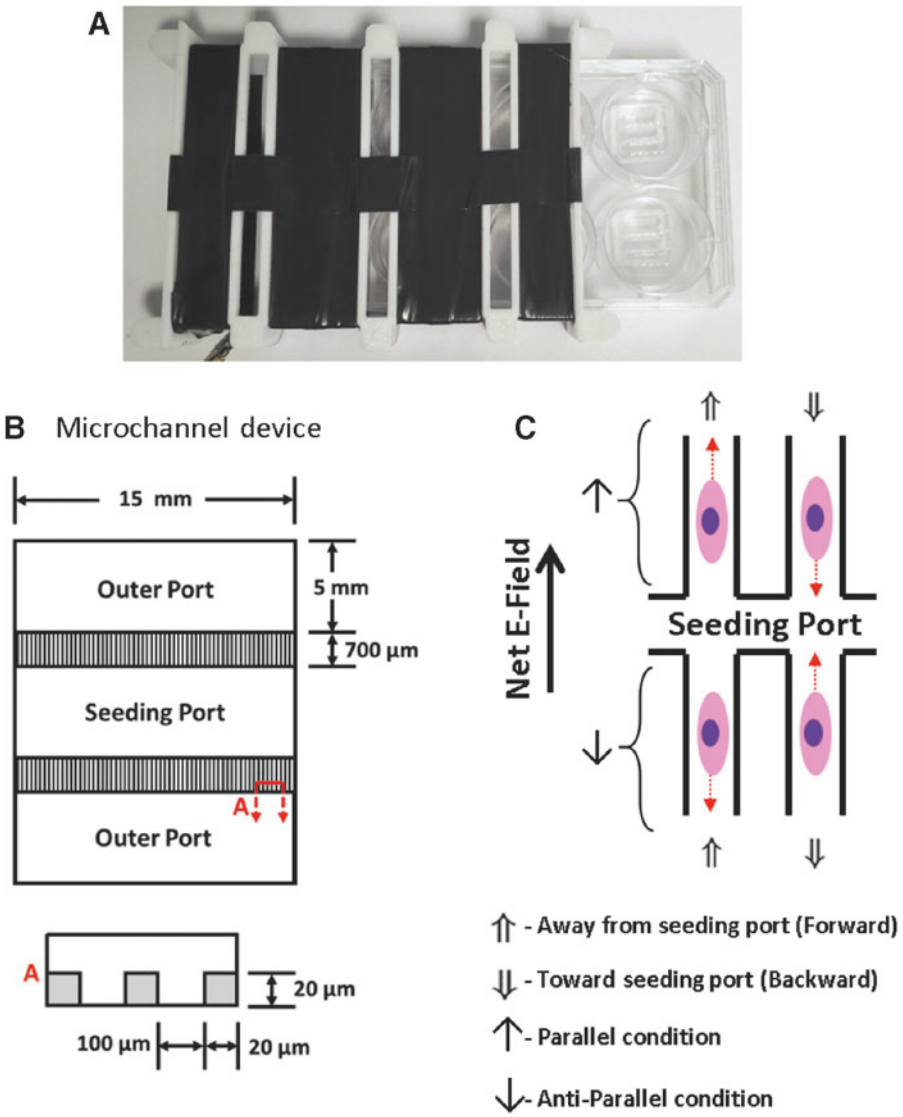

FIG. 1. **(A)** Photograph of the Helmholtz coil with a six-well culture plate partially inserted inside. Microdevices fit into each well of the plate. The black regions are windings of the Helmholtz coil taped to secure them. Supplementary Figure S1 shows further details in another schematic. **(B)** Schematic of microdevice used in migration experiments. **(C)** Directional labels for microchannel experiments. The migration direction of a cell is taken as parallel when moving in the same direction as the net direction of the electric field and antiparallel when moving against the net direction, as in Garg et al.[9] Forward moving cells are considered when moving away from the seeding port and backward or reverse when moving toward the seeding port.

We hypothesized that iEFs impact mitochondrial function and may explain previously reported cell migration characteristics such as average speed, persistence, and numbers migrated. To explore this idea, we measured SDH activity as a surrogate of mitochondrial oxidative phosphorylation and lactate dehydrogenase (LDH) activity as a surrogate of glycolysis, in lysates prepared from MDA-MB-231 and MCF10A cells exposed to iEF and/or EGF. We found that iEFs decrease SDH activity in MDA-MB-231 cells and increase LDH activity in MCF10A cells in the presence of EGF.

Materials and Methods

Cell line and reagents

The MDA-MB-231 breast adenocarcinoma cells stably expressing green fluorescent protein (provided by Luker Laboratory, University of Michigan, Ann Arbor, MI) were cultured in growth media (GM) comprising Dulbecco's modified eagle medium (DMEM) (Gibco™; 11-995-073) supplemented with 1% penicillin–streptomycin–glutamine (Gibco™; 10-378-016) and 10% fetal bovine serum (FBS, EF-0500-A; Atlas Biologicals).[19] Nontransformed mammary epithelial MCF10A cells (American Type Culture Collection), serving as a noncancerous standard, were cultured in GM comprising DMEM-F12 (Corning; 10-103-CV) supplemented with 1% penicillin–streptomycin (100 μg/mL, 15140122; Life Technologies), 5% Horse Serum (HS) (Life-Technologies; 16050-122, 1783307), 0.1% insulin (10 μg/mL, I1882; Sigma-Aldrich), 0.05% hydrocortisone (0.5 mg/mL, H0888; Sigma-Aldrich), 0.02% EGF (20 ng/mL, AF-100-15; Peprotech), and 0.01% cholera toxin (100 ng/mL, C8052; Sigma-Aldrich). The MCF10A cells were used as nontumor/nonmetastatic control.[9] For all experiments discussed in this article, migration media (MM) containing lower levels of serum was used. For the cancer cell line, MM consisted of the same components as GM with only 0.1% FBS rather than 10%. For the MCF10A cells, MM consisted of the same components as GM with only 0.1% HS and no supplemental EGF.

Electrotransductive migration apparatus

Weak, temporally asymmetric iEFs were applied using a Helmholtz-style coil (Supplementary Fig. S1) that encases multiwell plates with viewing access for imaging cell migration in real-time.[9] The ranges of EFs induced and magnetic fields applied by these coils were 20 μV/cm–1 mV/cm and 6–20 μT, respectively.[9] The Helmholtz-style coil was driven by sawtooth waveforms to induce asymmetric net iEFs as previously described.[9] The direction of the iEFs were defined as parallel if primarily in the direction of migration (i.e., higher time averaged strength) and antiparallel if primarily opposite to the direction of migration (Fig. 1 and Supplementary Fig. S2).[9]

Microfluidic bidirectional microtrack assay and methodology for retrospective analysis

The custom-designed microfluidic bidirectional microtrack (MBDM) assay was described previously and used to determine the average speed (averaged over the 12 h duration of the experiment) and persistence of MDA-MB-231 (and other) cells with and without EGF gradients.[9] The polydimethylsiloxane (PDMS) MBDM device consists of three ports connected by 700 μm long microchannels, each measuring 20 μm × 20 μm cross section (Fig. 1A), with individual devices plasma bonded to the PDMS-coated bottom surface of each well of a six-well multiwell plate that can be inserted into the Helmholtz-style coil apparatus (Supplementary Fig. S1). The microtracks were treated with fibronectin solution (10 μg/mL; Corning 354008, in 1 × phosphate-buffered saline) for 1 h at 37°C. Cell media was then added to the outer ports to completely fill the port. Then $\sim 2 \times 10^5$ cells were seeded in the center seeding port such that the media level remained below the outer ports. This prevented cells from flowing into the channels. The cells were allowed to attach for 12 h in MM in a 37°C incubator. Afterward, the cell media was aspirated and replaced with fresh MM in the seeding port. The outer ports were filled with MM with or without EGF (25 ng/mL). The cells were then incubated for 36 h, while the media was replenished every 12 h. This allowed for cells to start migrating into the microchannels before starting the experiments. After 36 h, the plate was imaged using a microscope (Nikon Eclipse TE2000-U) with an enclosed chamber that maintained a 37°C and 5% CO_2 environment. Images were recorded every 5 min over a 12 h period. The movies were then analyzed using Fiji,[20] extracting cell position at every time point utilizing a manual cell tracker plugin (MtrackJ plugin[21]).

The average speed data for migrating cells reported in Garg et al.[9] were based on an average over the entire 12 h duration of the experiment. Here, we examine the same data retrospectively by considering the speeds measured at discrete 30 min intervals. Monitoring over such short intervals provides a more ''instantaneous'' or momentary snapshot of the properties of migration. An array of speeds as well as directions is then ascribable to migrating cells, enabling a more accurate depiction of the migratory process. Such an approach is necessary as cells can at any given time, be stationary, moving forward (i.e., away from the central seeding chamber) or moving in the reverse direction (i.e., toward the central seeding chamber). This retrospective analysis enables the velocity (i.e., speed and direction) to be determined, with positive velocities signifying movement away from the seeding chamber and negative velocities indicating movement toward the seeding chamber.

At each 30 min time point, the net displacement of the cells is monitored by number of pixels, where each pixel corresponds to ~ 0.63 μm. A movement of five pixels over the 30 min duration then corresponds to a speed of about 0.1 μm/min. From the data reported in Garg et al.,[9] the natural logarithms (to enable discerning of differences) of the speeds are considered. The speeds were nondimensionalized by normalizing with the average speed in the control condition [iEF(−)/EGF(−)] for MDA-MB-231 cells and by the average speed in the EGF condition [iEF(−)/EGF(+)] for MCF10A cells since these cells do not migrate in the absence of EGF. All distributions are displayed as histograms normalized to yield a probability density function (pdf). The bin heights are calculated as the number of occurrences of a particular speed divided by the product of the total number of recorded speeds and speed bin width. For the histograms, a pdf, $f(\ln(\tilde{v}))$, is fit to the raw data using a maximum likelihood estimate. A normal (Gaussian) distribution is fit to all single-mode data, while a bimodal distribution of the form is fit for distributions that display obvious bimodality,

$$f(\ln(\tilde{v})) = \frac{p}{\sigma\sqrt{2\pi}} e^{-\frac{1}{2}\left(\frac{[\ln(\tilde{v})]-\mu}{\sigma}\right)^2} + \frac{(1-p)}{\sigma\sqrt{2\pi}} e^{-\frac{1}{2}\left(\frac{[\ln(\tilde{v})]-\mu}{\sigma}\right)^2}, \quad (1)$$

where $f\left(\ln(\tilde{v})\right)$ is the pdf, $\tilde{v}$ is the nondimensional speed, μ is the mean of the distribution, σ is the standard deviation, and p is a parameter that is best described as the probability that a particular speed will fall within the lower portion of the bimodal distribution. The parameter p is calculated as the area under the lower portion of the bimodal curve divided by the total area under the bimodal distribution. The values for these parameters are provided in the figure captions referred to in the ''Results'' section.

SDH and LDH activity assay

SDH and LDH activities were measured as indicators of metabolism by oxidative phosphorylation and glycolysis, respectively. Relative activities of SDH and LDH were assessed using enzymatic assays (MAK066 and MAK197; Sigma Aldrich). LDH is an enzyme involved in the interconversion between lactate and pyruvate and is detected in the assay by monitoring the associated production of the cofactor NADH from its oxidized NAD^+ state. SDH is the only enzyme involved in both the citric acid cycle and electron transport chain. In brief, cells (1×10^6) were then plated in each well of two 6-well plates in GM. After at least 3 h, the cell media was changed to MM for the respective cell line with or without 25 ng/mL of supplemental EGF. One plate was inserted into the Helmholtz coil apparatus while the other was placed on a separate shelf in the same incubator as control. The function generator was set to output a 100 kHz, 20 V_{pp} sawtooth waveform. After 12 h of treatment, the cells were trypsinized and collected. Both enzyme assays were performed as per manufacturer's standardized instructions. The final activities were normalized to protein content for each respective condition with the latter quantified using a Lowry-based method (Detergent Compatible Protein Assay; Bio-Rad) and are presented relative to control.

Statistical analysis

All statistical analyses were performed in IBM SPSS Statistics 27. LDH and SDH experiments contained $N = 3$. For LDH and SDH measurements, the data were tested with the one-way analysis of variance test followed by *post hoc* Tukey–Kramer Honestly Significance Difference method. Migration experiments were carried out for $N = 3$. For microchannel data, the data sets for ''percentage of time moving slow'', ''average forward speed'', and ''average backward speed'' were tested for normality using the Shapiro-Wilk test. None of the conditions was found to follow a normal distribution. The conditions were then compared using the Kruskal–Wallis H test with adjustment for ties followed by pairwise comparisons using the Dunn–Bonferroni approach, which adjusts for multiple groups. The probability density functions of momentary speeds in the microchannels were fit using MATLAB's built in maximum likelihood estimate function mle().

Results

iEFs reduce SDH activity in MDA-MB-231 cancer cells and increase LDH activity in nontransformed MCF10A epithelial cells

Glucose converted to pyruvate in the cytoplasm can enter mitochondria to undergo oxidative phosphorylation (a key step of which involves SDH to catalyze conversion of

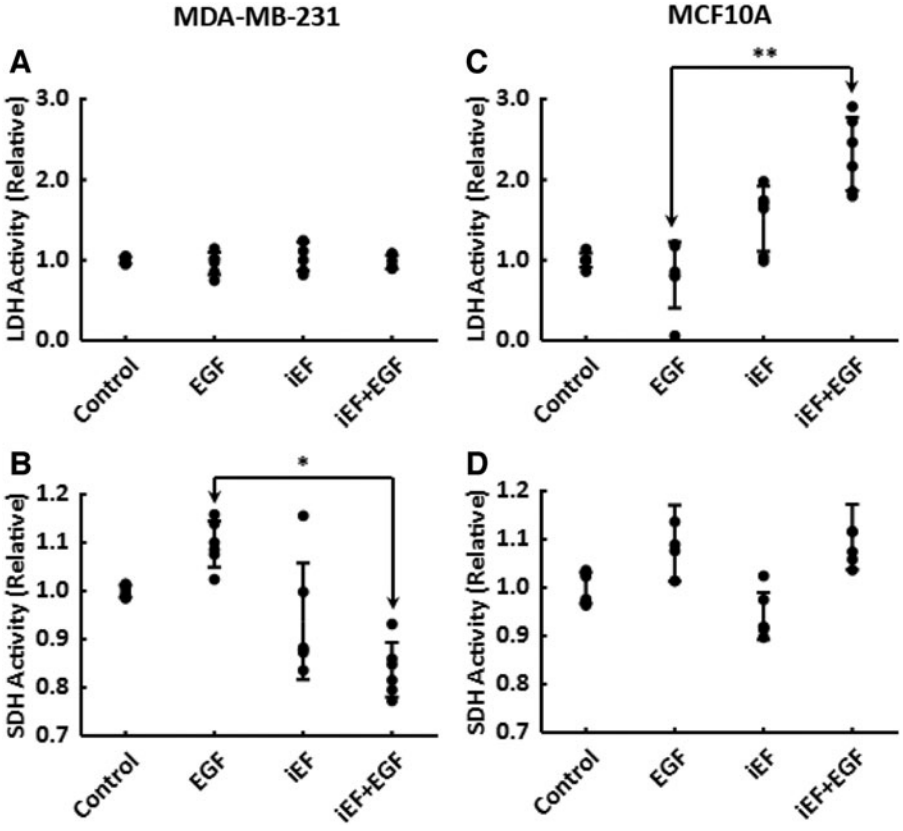

FIG. 2. LDH **(A)** and SDH **(B)** activities in MDA-MB-231 cells with and without iEF and EGF. LDH **(C)** and SDH **(D)** activities in MCF10A cells with and without iEF and EGF. Results are shown for $N = 3$ separate experiments (three separate six-well plates on separate days). Values have been normalized to the control condition. Black circles represent the calculated activities from each individual well across three experiments. Error bars represent one standard deviation above and below the mean. $*p < 0.05$. LDH, lactate dehydrogenase; SDH, succinate dehydrogenase; EGF, epidermal growth factor; iEF, induced electric field.

succinate to fumarate) or be converted to lactate in the cytoplasm, catalyzed by LDH.[22] Therefore, LDH and SDH activities are effective markers of whether a cell is relying more on glycolysis or rather on oxidative phosphorylation for its primary energy needs. SDH and LDH activities are shown in Figure 2 for MDA-MB-231 and MCF10A cells, with and without EGF and with and without iEFs. It can be seen from Figure 2A that there is no discernable change in LDH activity for MDA-MB-231 cells for all treatment conditions [EGF(+/–)/iEF(+/–)]. However, SDH activities are significantly downregulated (23.7% lower than EGF alone) by iEF in the presence of EGF for MDA-MB-231 cells, but not with iEF alone. This implies that oxidative phosphorylation in MDA-MB-231 cells is hindered in the presence of EGF.

In contrast to MDA-MB-231 cells, the SDH activity in nontransformed, MCF10A epithelial cells appears unaffected for all treatments [EGF(+/–)/iEF(+/–)] (Fig. 2D). However, LDH activity is observed to increase significantly in the presence of iEF and EGF (Fig. 2C). This implies that oxidative phosphorylation in MCF10A cells is unaffected or the change unmeasurable with this enzymatic assay, but that the glycolytic pathway is enhanced. This is in stark contrast to observations with the MDA-MB-231 cancer cell line, in which the glycolytic pathway seemed unaltered while oxidative phosphorylation was hindered. Interestingly, both cell lines exhibited statistically significant changes in enzyme activities only in the presence of EGF, indicating that EGF may enhance the electrotransductive mechanism by which iEFs interact with these cells.

iEFs have different effects on forward and reverse migration speeds in microtracks

The results reported previously[9] were based on average migratory behavior over the duration of the 12 h experiments. The data of Garg et al.[9] were examined retrospectively by

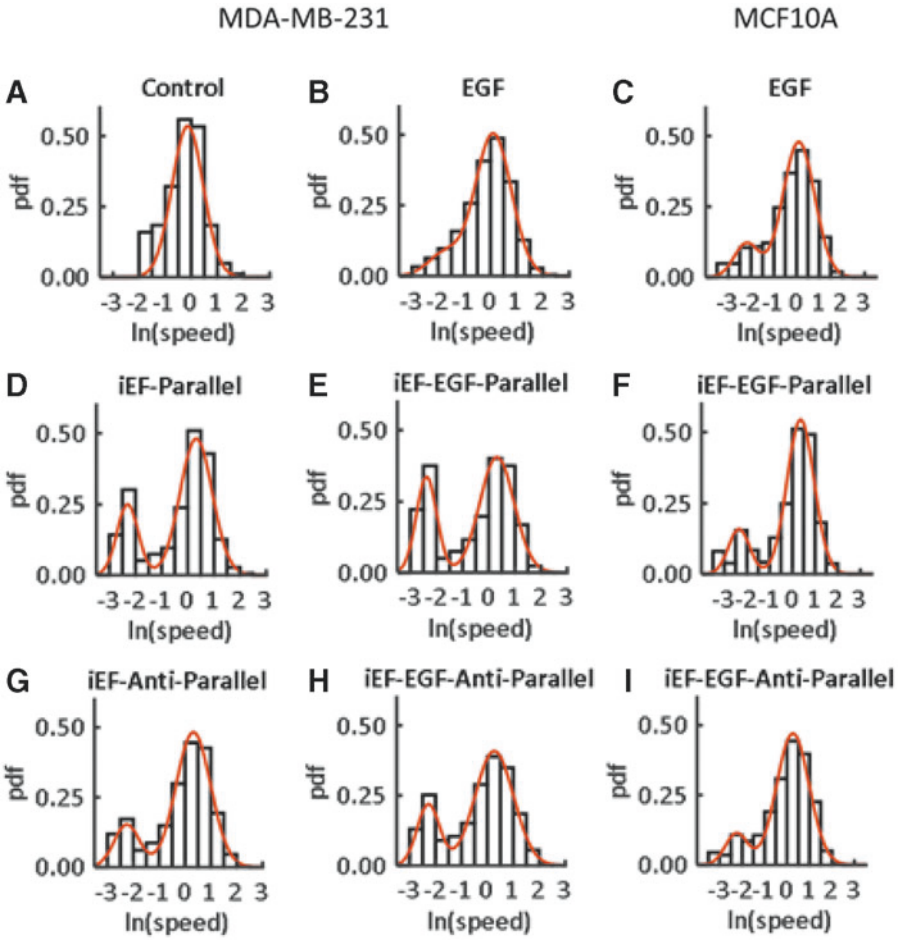

FIG. 3. pdfs for MDA-MB-231 and MCF10A cells for different conditions constructed from the momentary speed data sets from the MBDM assay of Garg et al.[9] All speeds were normalized by the average control [iEF(–)/EGF(–)] speed for MDA-MB-231 cells and the corresponding average control [iEF(–)/EGF(+)] speed for MCF10A cells. The red curves represent fits to Equation (1). The respective values of the parameters in Equation (1) are **(A)** $\mu = -0.242$, $\sigma = 0.719$; **(D)** $p = 0.255$, $\mu_1 = -2.305$, $\sigma_1 = 0.406$, $\mu_2 = 0.321$, $\sigma_2 = 0.618$; **(G)** $p = 0.187$, $\mu_1 = -2.255$, $\sigma_1 = 0.490$, $\mu_2 = 0.322$, $\sigma_2 = 0.672$; **(B)** $p = 0.129$, $\mu_1 = -1.752$, $\sigma_1 = 0.634$, $\mu_2 = 0.101$, $\sigma_2 = 0.690$; **(E)** $p = 0.330$, $\mu_1 = -2.379$, $\sigma_1 = 0.393$, $\mu_2 = 0.314$, $\sigma_2 = 0.660$; **(H)** $p = 0.237$, $\mu_1 = -2.278$, $\sigma_1 = 0.434$, $\mu_2 = 0.264$, $\sigma_2 = 0.745$; **(C)** $p = 0.125$, $\mu_1 = -2.990$, $\sigma_1 = 0.372$, $\mu_2 = -0.769$, $\sigma_2 = 0.720$; **(F)** $p = 0.144$, $\mu_1 = -3.043$, $\sigma_1 = 0.279$, $\mu_2 = -0.488$, $\sigma_2 = 0.615$; **(I)** $p = 0.105$, $\mu_1 = -3.046$, $\sigma_1 = 0.292$, $\mu_2 = -0.608$, $\sigma_2 = 0.755$;, where the subscript 1 refers to the left (lower speed) peak and 2 refers to the right (higher speed) peak. MDA-MB-231 cell numbers in each condition are $N = 190$, 100, 109, 242, 93, 95; MCF10A cell numbers in each condition are $N = 270$, 165, 127. pdf, probability density function; MBDM, microfluidic bidirectional microtrack.

analyzing momentary (i.e., measured at 30 min intervals) speeds and distributions, leading to further insight on how iEFs affect cell migration. Such an approach provides each cell with an array of velocities where a positive velocity denotes the forward direction or migration away from the seeding chamber, and a negative velocity signifies a reverse direction or movement toward the seeding chamber (Fig. 1B).

Figure 3 shows distributions for the momentary speeds of all cells for each condition. Interestingly, all iEF conditions show a clear bimodality compared with control [iEF(−)/EGF(−)] and compared with EGF alone [iEF(−)/EGF(+)]. An explanation for this bimodality is that there could be a subgroup of cells that are barely moving. However, the corresponding figure for the average speed (taken over 12 h) shows no such bimodality (Fig. 4), implying therefore that such a subgroup does not exist and that iEFs are instead causing an increase in instances of cells migrating slowly. This is evident in Figure 5, where the average amount of time a cell spends traveling slowly or is immobile (<0.1 μm/min) is significantly higher for the parallel iEF condition regardless of the presence of EGF. This finding agrees with the observed slower average migration speed in the iEF parallel condition but does not fully explain the higher observed speeds in the antiparallel conditions reported previously.[9]

The data, when further split into average forward and reverse speeds for each cell, reveal the histograms shown in Supplementary Figure S3, preserving the same bimodality observed in Figure 3. In Supplementary Figure S3, each cell contributes two average speeds, one for the forward direction and one for reverse. Interestingly, the bimodality is still present in all iEF cases and more pronounced in the presence of EGF. This suggests that cells are traveling much slower regardless of whether they are moving forward or in the reverse direction. Figure 6 shows the average forward and reverse speeds plotted separately. As can be seen from this figure, iEFs are actually significantly increasing the average forward speed while significantly decreasing the reverse speed (except for MCF10A cells with antiparallel iEF). The results in Figures 5 and 6 together contribute to a better understanding of the trends of average cell speeds previously reported and additionally provide insight into how these cells are affected by iEFs. Rather than directly affecting the average speeds, cells are actually able to increase their forward speed (regardless of direction of iEF) but struggle to initiate migration in the reverse direction. These periods when cells are moving extremely slowly (or not at all) occur more frequently in the presence of iEFs, and in a direction-dependent manner.

Discussion

Cell migration is an energy-intensive process and is an aspect of metastasis. Noncontact, weak iEFs (<100 μV/cm) have been shown to hinder the migration of highly metastatic MDA-MB-231 breast cancer cells by electrotransduction in the presence of growth factors and chemokines.[8,9] This hindrance is observed in numbers migrated as well as in the average speed, especially with migration under EGF gradients. In this work, a retrospective analysis of migration velocity data in

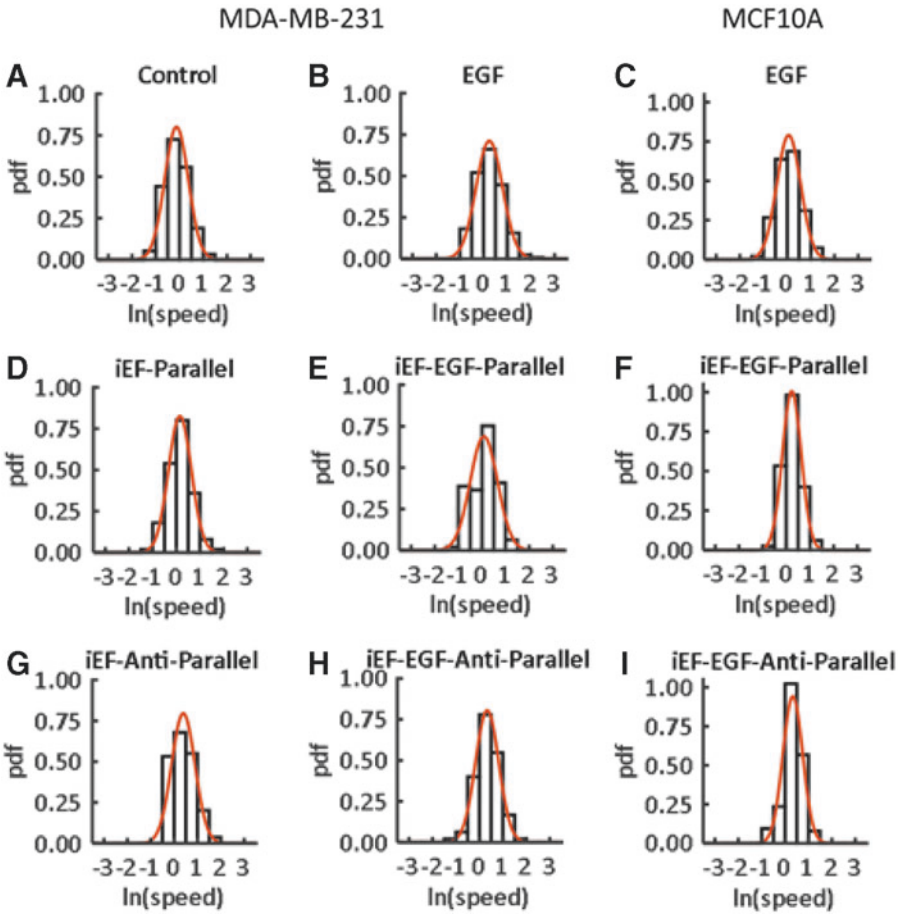

FIG. 4. pdfs for MDA-MB-231 and MCF10A cells for different conditions constructed from the average speed data sets (averaged over the 12 h duration of the experiments) from the MBDM assay of Garg et al.[9] All speeds were normalized by the average control [iEF(−)/EGF(−)] speed for MDA-MB-231 cells and the corresponding average control [iEF(−)/EGF(+)] speed for MCF10A cells. The red curves represent fits to Equation (1). The respective values of the parameters in Equation (1) are: **(A)** $\mu = -0.343$, $\sigma = 0.498$; **(D)** $\mu = -0.064$, $\sigma = 0.483$; **(G)** $\mu = 0.175$, $\sigma = 0.501$; **(B)** $\mu = 0.026$, $\sigma = 0.560$; **(E)** $\mu = -0.135$, $\sigma = 0.579$; **(H)** $\mu = 0.113$, $\sigma = 0.495$; **(C)** $\mu = 0.060$, $\sigma = 0.504$; **(F)** $\mu = 0.232$, $\sigma = 0.397$; **(I)** $\mu = 0.331$, $\sigma = 0.423$.

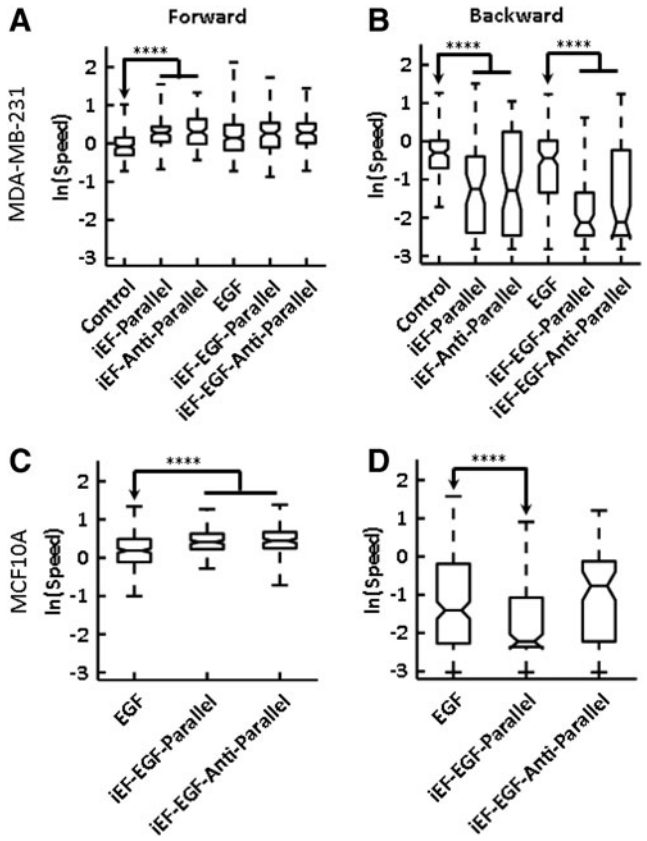

FIG. 5. Data from Garg et al.[9] are analyzed here after segregating occurrences of **(A)** forward (i.e., away from seeding chamber) speeds and **(B)** reverse (i.e., toward the seeding chamber) speeds for MDA-MB-231 cells, and **(C)** forward and **(D)** reverse speeds for MCF10A cells. $****p < 0.0001$.

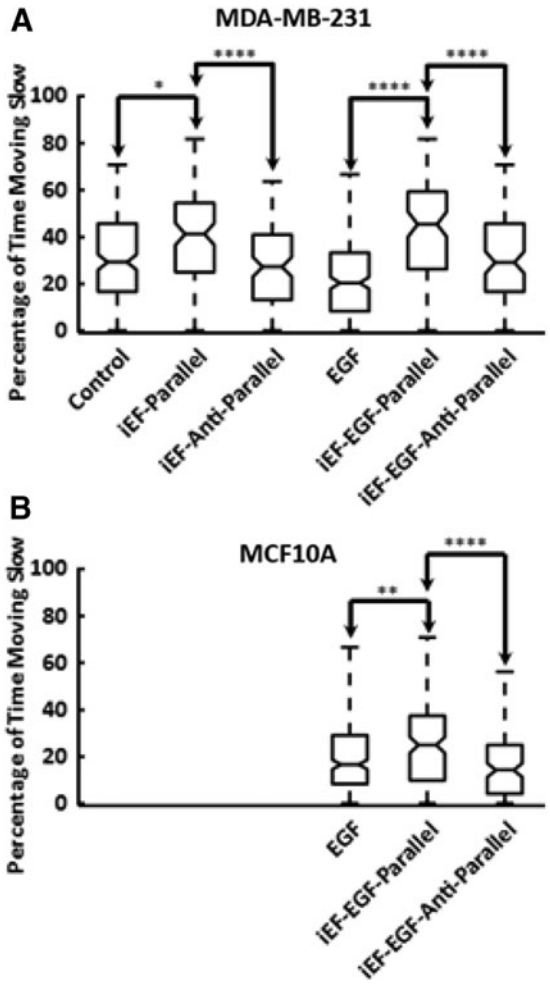

FIG. 6. Percentages of occurrences of slow speeds (<0.1 μm/min), including zero speeds, for **(A)** MDA-MB-231 cells and **(B)** MCF10A cells under various treatment conditions from the data of Garg et al.[9] $*p < 0.05$, $**p < 0.01$, and $****p < 0.0001$.

the MBDM assay revealed previously unknown details of cell migration under iEF treatment. We have also presented evidence that metabolic processes are also influenced by iEFs.

The effects of iEF on metabolism have not been previously explored. However, SK-BR-3 cells (Her-2 overexpressing breast cancer cell line) exposed to extremely low frequency electromagnetic fields (ELF-EMFs) have been reported to show a reduction in cell proliferation coupled with an increase in mitochondrial membrane potential and reduction in mitochondrial cytochrome c.[23] ELF-EMFs were found to enhance mitochondrial respiration, but in the absence of respirometry analysis to assess mitochondrial function, the results of Destefanis et al.[23] indicate characteristics of mitochondrial dysfunction and potential induction of cytochrome *c* release in the cytoplasm, which initiates apoptosis. Interestingly, no change in LDH activity was observed in their study.

We hypothesized that since PI3K/Akt signaling has been shown to regulate cellular metabolism of both glucose and glutamine[24] and also shown to interact with iEF,[9] there must be an accompanying metabolic effect from iEF. Since oxidative phosphorylation is the primary source of ATP generation, and ATP is the energy currency for cell migration, we explored SDH activity as an indicator of mitochondrial respiration. In MDA-MB-231 cells, we observed that SDH activity is reduced by iEF in the presence of EGF while LDH remains unchanged. Of note, baseline LDH activity in MDA-MB-231 cells tends to be high compared to normal MCF10A epithelial breast cells and iEF-induced changes may therefore not be detectable by this biochemical enzymatic assay.

This partial suppression of oxidative phosphorylation via reduced SDH activity may reflect metabolic reprogramming, and could explain the iEF-induced decrease in average migration speeds reported with the MBDM assay[9] and hindered migration observed in the Transwell assay in the presence of EGF-gradients.[8,9] However, these observed metabolic effects cannot on surface address the directional dependence of iEF. Reduced SDH activity may also explain the previously reported effects of iEF on the cytoskeleton.[8,9] With EGF gradients, iEFs were shown to render F-actin diffuse in the cytoplasm of MDA-MB-231 cells without directional polymerization in contrast to the directional protrusions formed in the absence of iEF. Drastic modification of the actin cytoskeleton has been previously reported with metabolic inhibition and ATP depleted conditions for different cells.[25–32] Therefore, we infer that the observed effects of iEF on modification of the actin cytoskeleton of MDA-MB-231 cells

may be linked to lowering of SDH activity in mitochondria and associated changes in ATP availability.

In contrast, LDH activity is increased by iEF in the presence of EGF in the nontransformed (normal) MCF10A breast epithelial cells, while SDH activity is either unchanged or changes undetectable using the enzymatic assay. Since LDH activity is an indicator of glycolysis, this result implicates iEFs as causing these cells to switch from their normally preferred reliance on oxidative phosphorylation to the less efficient glycolytic pathway. It is also possible that these cells draw on glycolysis in addition to oxidative phosphorylation (if SDH activities are indeed unchanged) to generate ATP, which may explain the recorded increase in average migration speeds with antiparallel iEFs.[9]

A key point is that the SDH/LDH activities measured in culture plates have no directionality (such as parallel or antiparallel iEFs) as in the case of the MBDM assay microtracks and provide a preliminary snapshot into metabolic differences that may be induced by iEF. We acknowledge that these assays do not comprehensively address iEF induced changes in metabolic activity and phenotype, but believe that there is scope to better understand the differential effect of iEF on metabolism by using real-time assays of metabolism such as using Seahorse Bioanalyzer and metabolomics, in the future. Nevertheless, our findings suggest that a reduction in average speed or numbers of MDA-MB-231 cells migrated and increases in average speed of MCF10A cells is linked with lowering of SDH activity in MDA-MB-231s and by increased flux through glycolysis as indicated by increased LDH activity in MCF10As. While this energy-based argument may explain effects of iEF on average and momentary speed and persistence, the reasons for directional dependence on iEFs remain enigmatic and needs to be explored further.

Conclusion

A retrospective analysis of the momentary speeds and velocities (forward and reverse directions) reported in Garg et al.,[9] revealed that cancer cell migration is hindered by iEFs because migrating cells slow down or are immobile some of the time in the 700 μm long microchannel over the duration of the experiment. Thus, iEFs not only reduce the number of cancer cells migrated but, on average, also slow them down. We have separately shown that SDH activity is hindered in MDA-MB-231 cells and LDH activity is enhanced in MCF10A cells by iEFs in the presence of EGF. This additional data on the effects of iEF on cellular metabolism may explain the previously reported changes in migration characteristics in microtrack microchannels. This work has paved the way for better understanding of how iEFs interact with MDA-MB-231 cells and points to possible new therapeutic options for treating metastasis that involve targeting specific metabolic pathways.

Authors Contributions

Conceptual design of the experiments was developed by T.H.J., A.A.G., K.K., J.W.S., R.K.G., and V.V.S. The coils and holders for the MBDM assay were designed and fabricated by T.H.J., and the design of the MBDM apparatus was led by A.A.G. Measurements of the coil currents were performed by T.H.J. and calculation of the induced EFs were carried out by T.H.J. The experiments were conducted by T.H.J., A.A.G., and K.K. The article was written by J.W.S., R.K.G., K.K., and V.V.S.

Author Disclosure Statement

No competing financial interests exist.

Funding Information

The publication was supported, in part, by National Institutes of Health grant R01CA109527 and Department of Defense breast cancer breakthrough awards W81XWH 1910088 to R.K.G. K.K.'s contribution was supported by Pelotonia Post-Doctoral Fellowship award. Opinions, interpretations, conclusions, and recommendations are those of the authors and are not necessarily endorsed by the Department of Defense. We also acknowledge funding from the Cancer Biology Program of The Ohio State University Comprehensive Cancer Center, which is supported by grant P30 CA016058, National Cancer Institute, The Ohio State University Materials Research Seed Grant Program, funded by the Center for Emergent Materials, an National Science Foundation Materials Research Science and Engineering Center, grant DMR-1420451, the Center for Exploration of Novel Complex Materials, and the Institute for Materials Research, and National Science Foundation (CBET-1752106). Additional funding was provided by Department of Mechanical and Aerospace Engineering (through the Future Academic Scholars Training or FAST Program) and The Center for Cancer Engineering at The Ohio State University. This work was also supported, in part, by the Mary Wieczynski Furnivall Cancer Research Fund.

Supplementary Material

Supplementary Figure S1
Supplementary Figure S2
Supplementary Figure S3

References

1. Nuccitelli R. A role for endogenous electric fields in wound healing. Curr Top Dev Biol 2003;58:1–26.
2. Friedl P, Alexander S. Cancer invasion and the microenvironment: Plasticity and reciprocity. Cell 2011;147:992–1009.
3. Levin M. Large-scale biophysics: Ion flows and regeneration. Trends Cell Biol 2007;17:261–270.
4. Lin B-J, Tsao S-H, Chen A, et al. Lipid rafts sense and direct electric field-induced migration. Proc Natl Acad Sci U S A 2017;114:8568–8573.
5. Li J, Lin F. Microfluidic devices for studying chemotaxis and electrotaxis. Trends Cell Biol 2011;21:489–497.
6. Wu D, Ma X, Lin F. DC electric fields direct breast cancer cell migration, induce EGFR polarization, and increase the intracellular level of calcium ions. Cell Biochem Biophys 2013;67:1115–1125.
7. Nakajima K-I, Zhu K, Sun Y-H, et al. KCNJ15/Kir4.2 couples with polyamines to sense weak extracellular electric fields in galvanotaxis. Nat Commun 2015;6:8532.
8. Ahirwar DK, Nasser MW, Jones TH, et al. Non-contact method for directing electrotaxis. Sci Rep 2015;5:11005.
9. Garg AA, Jones TH, Bushman S, et al. Electromagnetic fields alter the motility of metastatic breast cancer cells. Nat Commun Biol 2019;2:303.

10. Li Y, Yao L, Mori Y, et al. On the energy efficiency of cell migration in diverse physical environments. Proc Natl Acad Sci U S A 2019;116:23894–23900.
11. Zanotelli MR, Goldblatt ZE, Miller JP, et al. Regulation of ATP utilization during metastatic cell migration by collagen architecture. Mol Biol Cell 2018;29:1–9.
12. Tang S, Wang X, Shen Q, et al. Mitochondrial Ca^{2+} uniporter is critical for store-operated Ca^{2+} entry-dependent breast cancer cell migration. Biochem Biophys Res Commun 2015;458:186–193.
13. Cuddapah VA, Sontheimer H. Ion channels and transporters in cancer. 2. Ion channels and the control of cancer cell migration. Am J Physiol Cell Physiol 2011;301:C541–C549.
14. Wang Y, Zang QS, Liu Z, et al. Regulation of VEGF-induced endothelial cell migration by mitochondrial reactive oxygen species. Am J Physiol Cell Physiol 2011;301: C695–C704.
15. Zu XL, Guppy M. Cancer metabolism: Facts, fantasy, and fiction. Biochem Biophys Res Commun 2004;313:459–465.
16. Baysal BE, Ferrell RE, Willett-Brozick JE, et al. Mutations in SDHD, a mitochondrial complex II gene, in hereditary paragandlioma. Science 2000;287:848–851.
17. Gottlieb E, Tomlinson IPM. Mitochondrial tumour suppressors: A genetic and biochemical update. Nat Rev Cancer 2005;5:857–866.
18. Li P, Liu Y, Liu W, et al. IR-783 inhibits breast cancer cell proliferation and migration by inducing mitochondrial fission. Int J Oncol 2019;55:415–424.
19. Song JW, Cavnar SP, Walker AC, et al. Microfluidic endothelium for studying the intravascular adhesion of metastatic breast cancer cells. PLoS One 2009;4:e5756.
20. Schindelin J, Arganda-Carreras I, Frise E, et al. Fiji: An open-source platform for biological-image analysis. Nat Methods 2012;9:676–682.
21. Meijering E, Dzyubachyk O, Smal I. Methods for cell and particle tracking. Methods Enzymol 2012;504:183–200.
22. Vasan K, Werner M, Chandel NS. Mitochondrial metabolism as a target for cancer therapy. Cell Metab 2020;32: 341–352.
23. Destefanis M, Viano M, Leo C, et al. Extremely low frequency electromagnetic fields affect proliferation and mitochondrial activity of human cancer cell lines. Int J Radiat Biol 2015;91:964–972.
24. Koundouros N, Poulogiannis G. Phosphoinositide 3-kinase/Akt signaling and redox metabolism in cancer. Front Oncol 2018;8:160.
25. Korn ED, Carlier M-F, Pantaloni D. Actin polymerization and ATP hydrolysis. Science 1987;238:638–644.
26. Kuhne W, Besselmann M, Noll T, et al. Disintegration of cytoskeletal structure of actin filaments in energy-depleted endothelial cells. Am J Physiol 1993;264(5 Pt 2):H1599–H1608.
27. Atkinson SJ, Hosford MA, Molitoris BA. Mechanism of actin polymerization in cellular ATP depletion. J Biol Chem 2004;279:5194–5199.
28. van der Honing HS, Emons AMC, Ketelaar T. Actin based processes that could determine the cytoplasmic architecture of plant cells. Biochim Biophys Acta 2007; 1773:604–614.
29. Boldogh IR, Pon LA. Interactions of mitochondria with the actin cytoskeleton. Biochim Biophys Acta 2006;1763:450–462.
30. Ranjith P, Mallick K, Joanny J-F, et al. Role of ATP-hydrolysis in the dynamics of a single actin filament. Biophys J 2010;98:1418–1427.
31. Du J, Zhang L, Yang Y, et al. ATP depletion-induced actin rearrangement reduces cell adhesion via p38 MAPK-HSP27 signaling in renal proximal tubule cells. Cell Physiol Biochem 2010;25:501–510.
32. Shekhar S, Pernier J, Carlier M-F. Regulators of actin filament barbed ends at a glance. J Cell Sci 2016;129:1085–1091.

Address correspondence to:
Vish V. Subramaniam, PhD
Department of Mechanical and Aerospace Engineering
The Ohio State University
Columbus, OH 43210
USA

E-mail: subramaniam.1@osu.edu

Jonathan W. Song, PhD
Department of Mechanical and Aerospace Engineering
The Ohio State University
Columbus, OH 43210
USA

E-mail: song.1069@osu.edu